2nd Year Final Report

Nanogenerators For Self-Powered Nanodevices

Project funded by

Samsung Electronics Co., Ltd. (SAIT)

Date	June/2011
Organization	Georgia Institute of Technology
Department	Material Science & Engineering
Authors	**Zhong L. Wang**, Minbaek Lee

1. Research goal (2nd year of the project)

Goals
'Nanogenerators For Self-Powered Nanodevices'
Sub- task 1)
Storage of powers from nanogenerators using high-efficient supercapacitors
Sub- task 2)
Flexible nanogenerator- solar cell energy generation hybrid devices
Sub- task 3)
Wearable energy harvesting and storage system
Sub- task 4)
All-in-'ZnO NW' based Energy Store Package
Sub- task 5)
Nanogenerator Using Laterally Packaged Nanowire Arrays
Sub- task 6)
Piezo-phototronics – a new field

Table of contents

2. Background

The principle and technology demonstrated here have the potential of converting mechanical movement energy (such as body movement, muscle stretching, blood pressure), vibration energy (such as acoustic/ultrasonic wave), and hydraulic energy (such as flow of body fluid, blood flow, contraction of blood vessel) into electric energy that may be sufficient for self-powering nanodevices and nanosystems. The prototype technology established by the DC nanogenerator set a platform for developing self-powering nanosystems with important applications in implantable in-vivo biosensing, wireless and remote sensing, nanorobotics, MEMS, sonic wave detection and more.

In comparison to bulk materials, the nanowire based nanogenerators have a few key advantages. First, the degree of bending and elastic limit of nanowires are orders of magnitude higher than either thin film or bulk. They can suffer huge deformation without fracture. Second, nanowires are dislocation free and highly resistive to fatigue. The life time of the device is expected to be long. Third, the ZnO nanowires can be grown on any substrate at low temperature and low cost, thus, they can be integrated with substrates such as glass, polymer and metal foils. Fourth, nanowires can be bent by a tiny force. This allows the harvesting of energies created by tiny mechanical disturbance, such as air flow. Finally, ZnO is a biocompatible and environmentally green material, a large scale application of which will not produce any hazardous materials.

This project aims to expand technology of nanogenerators and piezotronic devices to explore new horizon of nanotechnology and nano-science. One of key ideas for this 2nd year is “wearable energy harvesting and storage system” using ZnO nanowires. On growing demand of portable energy system, clothes we wear everyday can afford the enough area to harvest energy from environment. Therefore, people can recharge their portable gadgets by simply connecting them to their energy harvesting clothes. Many existing energy harvesting and storage devices are still too bulky and heavy for intended applications. For example, high efficiency dye-sensitized solar cells (DSSCs) are employing fluorine-doped tin oxide (FTO) glass as the substrate of working electrode. However, the use of rigid FTO glass has restricted DSSC’s adaptability during transportation, installation, and application, requiring further development of flexible cells to improve DSSC’s adaptability.

Recently, our group at Georgia Tech and Samsung was able to demonstrate novel hybrid energy device based on unique ZnO nanowire-polymer fiber hybrid structure. The unique architecture of graphene electrodes and use of ZnO NWs as active material could be useful for the future development of flexible and wearable electronics. It would be applicable to develop fiber-based devices in a future such as fiber-based micro-batteries when flexibility and stretchability are required.

3. Details of achievements in 2nd Year

1) Novel fiber-based electrochemical storage devices

Sub- task 1) Storage of powers from nanogenerators using high-efficient supercapacitors. **Sub- task 3)** Wearable energy harvesting and storage system.
Related Deliverable: SCI Paper: 1 (*Published*)

(a) Abstract

Fiber supercapacitors presented in this section could be combined with the fiber nanogenerators, possibly enabling us to achieve "wearable power" system. In the future nanosystem, it will be necessary to store energy especially when intermittent energy source (such as ZnO-based nanogerators) is used. Fiber supercapacitors could enable us to store electrical energy that converted from mechanical energy by simple mechanical vibration such as light wind, footsteps, and heartbeats.

(b) Device structure and fabrication process

Our fiber supercapacitors are comprised of two electrodes, which employed a flexible plastic wire and a Kevlar fiber as a substrate. Both wire and fiber are covered with arrays of high-quality ZnO NWs grown by hydrothermal method, and ZnO NWs on the Kevlar fiber was coated with thin Au film to improve the charge collection capacity. The schematic of fiber-based electrochemical capacitors is illustrated in Figure 1c. The capacitor was assembled by entangling a plastic wire covered with NWs around a Kevlar fiber covered with Au coated NWs. For the entangling process, the plastic wire was placed on a stage, and the Kevlar fiber was entangled carefully by using tweezers. The resistance of the device was monitored during the entangling process to ensure the two electrodes were not in contact each other. As shown in the results of electrochemical measurements below, the liquid or gel electrolytes seem to play a role to separate the two electrodes, and the occasions of contact of the two electrodes were very rare in the devices with the electrolytes.

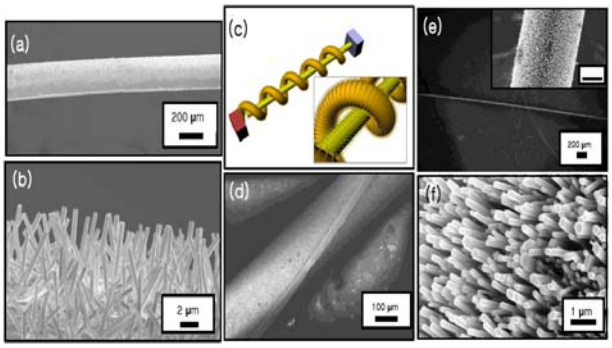

Figure 1

The typical number of turns of twisting Kevlar fiber around plastic wire was 5, and the active length of the plastic wire in which the plastic wire and Kevlar fiber are entangled to form the supercapacitor was 5 mm.

(c) Electrochemical property characterization in KNO_3 liquid electrolytes

The electrochemical properties of our capacitors in 1 M KNO_3 aqueous electrolyte solution were characterized using a potentiostat/galvanostat (Princeton Applied Research VersaStat 3F). Cyclic voltammetry shows good electrochemical stability and capacitance of fiber-based electrochemical capacitors. The scan range is between 0 and 500 mV with scan rates of 5, 20, 100 mV/s. The galvanostatic charge-discharge measurement was also conducted to characterize the electrochemical capacitor performance of the fiber supercapacitors. This area specific capacitance curve reveals that the specific capacitance of fiber supercapacitors in 1M KNO_3 reached up to ~ **0.21 mF/cm^2** at the voltage scan rate of 100 mV/s.

(d) Enhancement of the capacitances compared to ZnO NWs using MnO_2 coatings

In order to enhance specific capacitance of fiber-based supercapacitors, we coated ZnO NWs-grown plastic wires with MnO_2 to employ MnO_2's large pseudocapacitances. MnO_2 was successfully deposited onto ZnO NWs-grown plastic wire via the reduction of MnO_4- by ethanol at room temperature. First, 6 ml of 0.1 M KMnO4 solution was prepared in the vial. The ZnO NWs-grown wire was cut into appropriate size (9 mm) and put into the vial. Ultrasonication was performed to obtain better dispersion. Then, 6 ml of ethanol was added into a vial drop-wise under vigorous ultrasonication, and samples were taken out after 15 min. As shown in Figure 2, the specific capacitance of this energy storage device reached up to 2.0 mF/cm^2 at 100 mV/s, which is comparable to values reported for electrochemical micro-supercapacitors in the literature (0.4 ~ 2 mF/cm^2) as mentioned above. Figure 2 also shows that MnO_2 coating significantly enhanced specific capacitances (e.g. over 20 times increase of area specific capacitance after MnO_2 coating). This result indicates that the performance of our fiber supercapacitors could be further enhanced by using optimized MnO_2 coating.

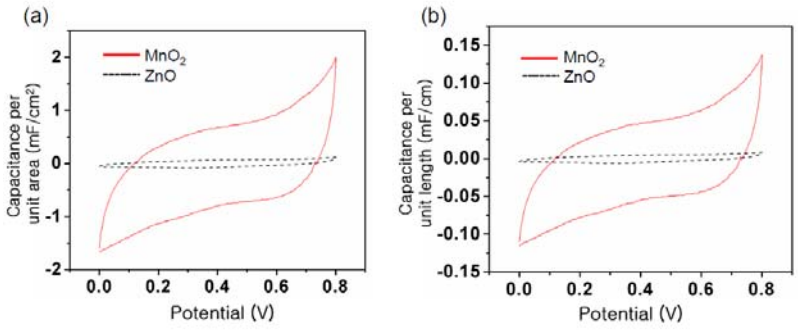

Figure 2

(e) Comparison of the performances of supercapacitor using three different configurations

The comparison of specific capacitances of fiber supercapacitors with three different configurations (ZnO NWs in two different electrolytes of KNO_3 and PVA/H_3PO_4, and MnO_2 coating in Na_2SO_4 electrolyte) is presented in Figure 3. Under the same device scheme and fabrication process as fiber supercapacitors with KNO_3, the gel electrolytes (PVA/H_3PO_4) resulted in a specific capacitance (2.4 F/cm^2) 10 times higher than the aqueous electrolytes (0.21 F/cm^2) at the voltage scan rate of 100 mV/s. We note that gel electrolyte is much more convenient than any aqueous electrolytes such as KNO_3 when the electrolytes need to be encapsulated in the future development of fiber supercapacitors. The gel electrolyte has also demonstrated higher specific capacitances compared to MnO_2-coated ZnO NWs in 1M Na_2SO_4 solution (2.0 mF/cm^2). This observation and higher specific capacitances using the gel electrolytes suggest that the gel electrolytes not only could be useful for fully wearable fiber supercapacitors, but also be promising to achieve high-efficient fiber supercapacitors**.**

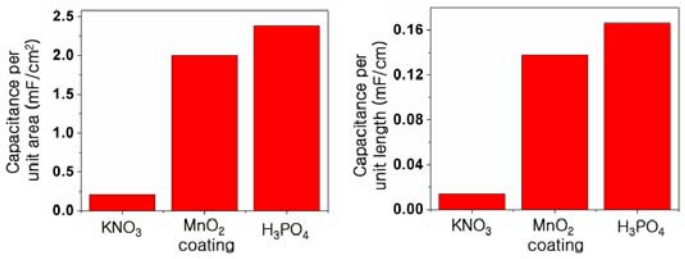

Figure 3

2) Fiber-based hybrid device composed of nanogenerator, supercapacitors and solar cell

Sub- task 1) Storage of powers from nanogenerators using high-efficient supercapacitors. **Sub- task 2)** Flexible nanogenerator- solar cell energy generation hybrid devices. **Sub- task 3)** Wearable energy harvesting and storage system.
Related Deliverable: SCI Paper: 1 (A*ccepted*)

(a) Abstract

We demonstrated the first integration of multiple energy harvesters and storage device along a single fiber suing ZnO nanowires (NWs) and graphenes as the basic materials, which allows a simultaneous harvesting of solar and mechanical energies. The unique architecture of fiber-based electrodes, use of ZnO NWs, and graphenes as active material and electrodes, could be useful for the future development of flexible and wearable electronics. In addition, the methodology demonstrated here would be applicable to develop other fiber-based electronic circuits or power-shirt when flexibility and stretchability are required.

(b) A novel structure of fiber-based hybrid device

The design of the power fiber is presented in Figure 1, which includes a nanogenerator, a DSSC and supercapacitor, all of which are built along one micro-size fiber. The radially grown ZnO nanowires (NWs) are the acting units for the nanogenerator (NG) that harvests mechanical energy and the core of the DSSC as well as the supercapacitor (SC) with large surface area. Graphene is used as the cylindrical electrodes for NG, DSSC and SC. The entire fabrication was based on a single polymethyl methacrylate (PMMA) fibre of diameter ~ 220 μm. The surface of the fibre was first covered by a layer of Au to serve as a common electrode. Then, quasi-aligned ZnO NW arrays were grown by a chemical approach. These structures are shared by the three devices to be built one by one. Inset of figure 1 shows a low magnification SEM image of a plastic wire covered with ZnO NWs. The close-up view on the NWs is shown in the inset in Figure 1. The as-grown ZnO NWs on the plastic wire show typical hexagonal flat ended, indicating their growth direction being c-axes. The diameters of a NW range from 500 to 700 nm, and the lengths are about 6 μm. Copper meshes covered with graphene were employed as distinct electrodes for each energy harvesting and storage devices, which were carefully wrapped around the fiber. The resistance of the device was monitored during the entangling process to ensure the two electrodes were not in contact with each other. After the plastic wire covered with ZnO NWs and graphenes on Cu mesh were prepared, our multi-energy devices have been fabricated by wrapping graphenes around the plastic wire (Figure 1). For DSSC part and supercapacitor part, liquid electrolyte and gel electrolyte were filled in between Cu mesh and the plastic wire for DSSC and supercapacitor part, respectively.

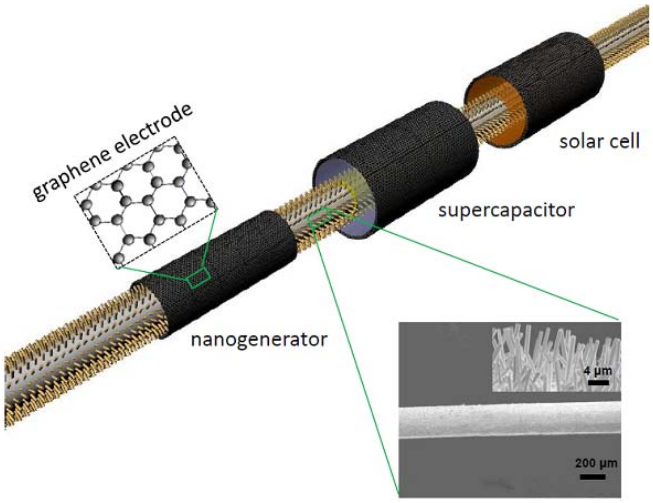

Figure 1

(c) Characteristics of fiber-based nanogenerator with a graphene electrode

The first device built on the fiber is a nanogenerator that converts mechanical energy into electricity with the use of piezoelectric property of ZnO. The size of the nanogenerator part is about 5 mm long. We measured the current output generated from the nanogenerator part using graphene as the top electrode by applying a pushing force. Manually driven pushing action (~ 5 Hz) delivered a shear stress between ZnO NWs and graphene electrode with a strain of ~0.1 %, which resulted in periodic friction motions between NWs and electrode. As shown in Figure 2c, the short-circuit current was successfully detected with sharp current peaks in responding to the mechanical agitation. The maximum output current from the nanogenerator was approximately 2 nA. Maximum open-circuit voltage was also measured to be about 7 mV (Figure 2d). The high carrier mobility (μ_c= 1760 $cm^2W^{-1}S^{-1}$) of the graphene electrode may have contributed to the high on/off ratio of the nanogenerator part of our multi-energy devices.

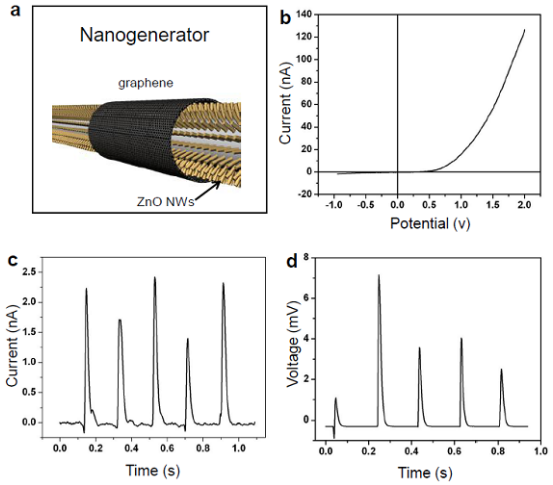

Figure 2

For a working nanogenerators, there must be a Schottky barrier at the contact between ZnO NWs and the top electrode. The ZnO NWs grown on plastic wire in our experiments were oriented along the c-axis. The work function of the graphene electrode is measured to be 4.4–4.7 eV. Since the electron affinity of ZnO is 4.1-

4.35 eV, a Schottky contact is formed at the interface between graphene and a ZnO NW (Figure 2b).

(d) Characteristics of fiber-based DSSC with a graphene electrode

DSSC is the second device fabricated around the fiber with the use of high quality graphene with good transparency. Thermal and chemical stabilities of graphenes also make them attractive as an alternative to the conventional metal oxide window materials for DSSCs. Based on the structure shown in Figure 1, the dye molecules are placed in between ZnO NWs and the bottom electrode on the fiber. A liquid electrolyte was injected between the fiber and the top graphene electrode. Since the dye is in liquid form, eventually it will be mixed up with the liquid electrolytes in between ZnO NWs and the bottom electrode. The electrolyte has to be effective to separate the two electrodes. The effective length and area of the plastic wire wrapped with graphenes were 5 mm, and 0.035 cm^2, respectively. Figure 3c shows plot of current density as a function of voltage (*J*-*V* curve). The short-circuit current density J_{sc}, open-circuit voltage V_{oc} were determined to be 0.35 mA/cm^2, and 0.17 V, respectively. The fill factor FF was 0.39. Hence, the energy conversion efficiency is 0.02 %. The low energy conversion efficiency is mainly attributed to the use of Cu mesh that is not fully transparent, resulting in a significant loss in the transfer of light energy to the dyes. To improve the DSSCs performance, graphenes on the transparent substrates or direct packaging of graphenes in the DSSCs without any substrates would be necessary.

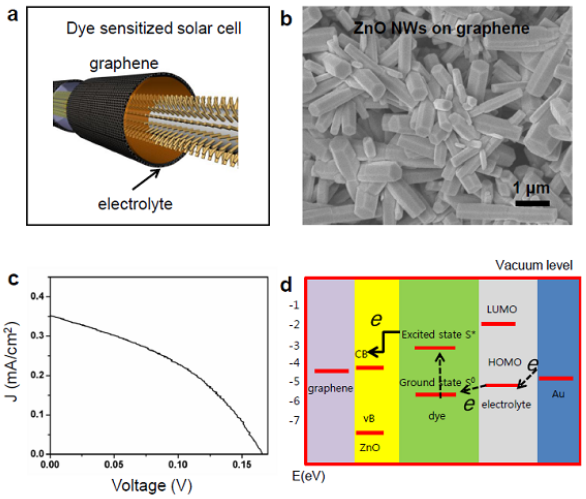

Figure 3

(e) Characteristics of fiber-based supercapacitor with a graphene electrode

The supercapacitor part is comprised of two electrodes, which employed a ZnO NWs on the plastic wire and graphenes on Cu mesh, with polymer gel electrolyte (PVA/H_3PO_4) filled between. While most electrolytes in electrochemical devices are in the liquid form, solid gel electrolytes have been recently explored as alternative electrolytes. Solid gel or polymer electrolytes were reported to combine the separator and the electrolyte into a single layer while liquid electrolytes require a separator to avoid electrical contact between the electrodes. In order to make our fiber-based energy devices with supercapacitors fully wearable, the electrolytes need to be fully encapsulated in the devices without any leakage. In this regards, using of solid gel electrolytes are more preferable than any conventional liquid electrolytes such as KNO_3 or H_2SO_4 for future applications of

our fiber multi-energy device.

Cyclic voltammetry from the supercapacitor part shows good electrochemical stability and capacitance of fibre-based electrochemical capacitors (Figure 4b). The scan range is between 0 and 250 mV with scan rates of 100 mV/s. From Figure 4b, the capacitance as a function of potential at a voltage scan rate of 100 mV/s can be easily obtained, and is shown in Figure 4c. The area specific capacitance can be calculated from cyclic voltammograms (Figure 4b) using the equation of $C = Q/V/A = I/S/A$, where C is the capacitance (F), Q is the charge (C) accumulated in the capacitors, V is the potential (V) in CV curve, I is the current (A) in CV curve, S is the voltage scan rate (V/s), and A is the effective area of supercapacitor (0.035 cm^2). The calculated area specific capacitance is shown in the upper part in Figure 4c. This area specific capacitance curve reveals that the specific capacitance of fiber supercapacitors reached up to ~ 0.4 mF/cm^2 at a voltage scan rate of 100 mV/s. Micro-supercapacitors were reported to demonstrate an area specific capacitance of 0.4 ~ 2 mF/cm^2, indicating that the capacitance value of 0.4 mF/cm^2 of our device is slightly lower than those in the literature. Further optimization would be necessary to increase the specific capacitances of fiber supercapacitors. For instance, matching the pore sizes and solvated ion sizes of electrolytes, and controlling the density of ZnO NWs is very critical to obtain the high performance of electrochemical capacitors. The conventional capacitors have two-dimensional plate-like substrates. Since our fiber supercapacitors possess unique one-dimensional shape substrates, capacitance per unit length (mF/cm) would be a useful parameter to characterize the capacitance behavior of the devices. In this regard, we calculated the capacitance per unit length by dividing the capacitance in Figure 4c by the effective length of the device (5 mm). The bottom figure in Figure 4c reveals that the capacitance per unit length reached up to about 0.025 mF/cm. The galvanostatic charge-discharge measurement was also conducted to characterize the electrochemical capacitor performance of the fiber supercapacitors, and the curve is shown in Figure 4d. To obtain this curve, charge-discharge current was kept constant at 1 μA. A typical triangular shape of these charge-discharge curves suggests that the capacitance of our fiber supercapacitors is originated from the effective ion adsorption at the interface of electrolyte/ZnO NWs.

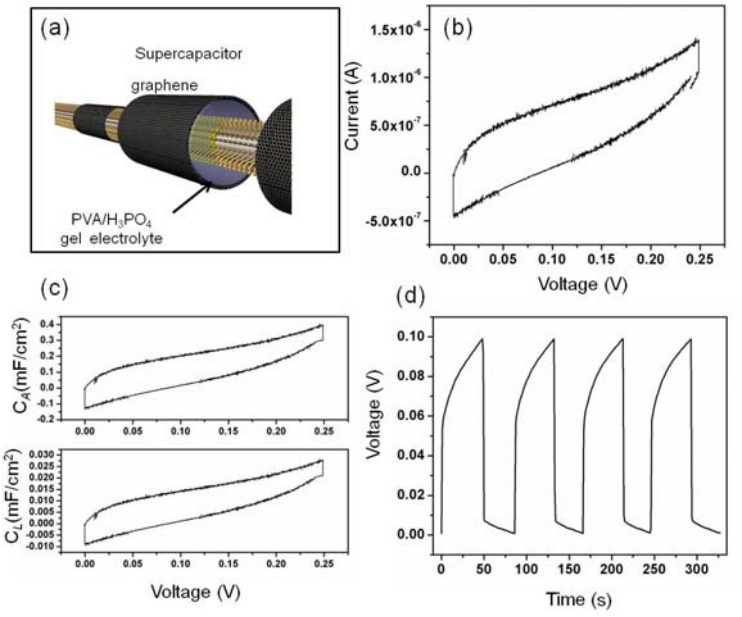

Figure 4

3) Position Control of wave guiding micro/nanowire using Converted Piezoelectric Effect

Sub- task6) Piezo-phototronics – a new field
Related Deliverable: Patent: 1 (*filing*)

(a) Abstract

We propose piezo-phototronics which is unique coupling of properties of ZnO NW. Electric field can induce transverse deflection of a single-crystal, free-standing ZnO microbelt as a result of converse piezoelectric effect. Moreover, ZnO nanowire can be utilize as wave guiding materials because of its refractive index. Coupling of two behaviors allows us to an attractive concept which is presented.

(b) Design of a unique device

Figure 1 shows a schematic diagram depicting the structure of a device. ZnO nanowires or even micro-wire can be utilized in this experiment. One end of wire was fixed to serve input window of light signal and counter end was allowed to be moved which resulted in changing the direction of light propagation. Two electrodes were designed to possibly apply high voltage with perpendicular to c-axis of ZnO wire. As a result, externally applied electric voltage may enable to bend the wave guiding nanowire/micro-wire with analog way.

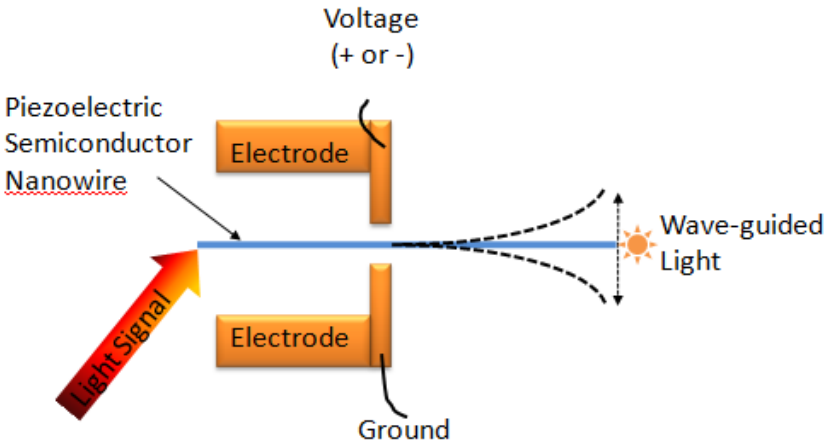

Figure 1

(c) Simulation of the deflection of piezoelectric wire (*adapted from* ***Ref. 1***) and experiment result of wave guide

We can utilize the finite element method (FEM) to calculate the response of a ZnO belt to an electric field applied perpendicular to the c-axis. The mechanical property of ZnO is E = 129.0 GPa and ν =

0.349, the relative dielectric constants are κ_{11}= 7.77 and κ_{33} = 8.91 for bulk ZnO, and the piezoelectric constants are e_{31} = -0.51 C/m^2 , e_{33} = 1.22 C/m^2 , and e_{15} = -0.45 C/m^2. A voltage of +100 V is applied uniformly through the two electrodes along the x-direction across the width of the microbelt. In the simulation, the two outer surfaces of the two electrodes perpendicular to the x-axis are set to be mechanical fixed, but all of the other surfaces and boundaries are free to relax/move to a mechanical equilibrium state. First, when a voltage of 100 V is applied along the x-direction (bE) $E_1$1^), according to eq 1, the converse piezoelectric effect will introduce a shear stress in the x-z plane (e.g., a-c plane) owing to e15 coupling,

$$\begin{cases} \sigma_p = c_{pq}\varepsilon_q - e_{kp}E_k \\ D_i = e_{iq}\varepsilon_q + \kappa_{ik}E_k \end{cases} \qquad (1)$$

The strain concentrates at the bottom of the belt near the electrodes, changing from tensile into compressive along the direction of the electric field. The effect of the shear strain is equivalent to applying a force in the x-z plane, which at least has a component that is perpendicular to the nanobelt. The force decays with the increase of the distance from the nanobelt root, but a small torque is created in the x-z plane. The microbelt has a high flexibility, and the strain at the root of the belt introduces a bending, resulting in a lateral deflection along the x-direction, as shown in Figure 2b, in which the deflection of the microbelt has been magnified by 100× to visually illustrate the effect. Although, the strain directly induced by the converse piezoelectric effect is small, the transverse deflection is amplified by the large aspect ratio of the microbelt. In our model, the 50 μm long belt has a maximal transverse deflection of 80 nm at the top. In fact, the practical belt has much higher aspect ratio. The length could extend to several millimeters. Thus, the resulting x-displacement could be close to 1 μm. The deflection angle of the microbelt has been calculated to be 0.1°, which does not depend on the actual length of the belt. Finally, it should be mentioned that from the simulations for different applied voltages, we found that there is a linear relationship between the deflection angle and the applied voltage. Also, when the applied voltage changes its sign, the deflection will change its direction.

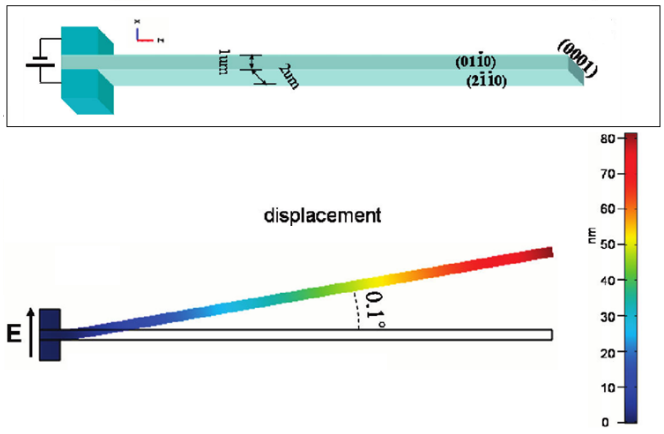

Figure 2

Aside from the deflection of nano-/micro-wire, we have conducted the experiment of wave guide on ZnO fine wire. Figure 3 shows photograph image of the employment of ZnO fine wire as a waveguide and inset of figure 3 shows a microscope image of ZnO fine wire utilized for this experiment. Fisrt, we illuminated reddish laser light on the one end of ZnO fine wire (left red dot in Figure 3) and successfully observed light output the other end of wire. It indicates that ZnO nano-/micro-wires can serve as a waveguide for optical application in a future. By employing piezoelectric effect of ZnO, one can make a wave guiding micro-/nano-electronics with capability of controlling their propagation.

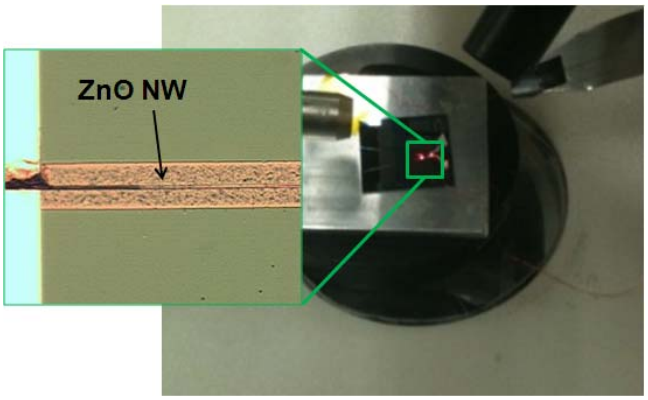

Figure 3

5. Publication & Patent

(a) Publication

Title	Author	Journal	vol. page
Fiber Supercapacitors Made of Nanowire-Fiber Hybrid Structures for Wearable/Flexible Energy Storage	Joonho Bae,Min Kyu Song, Young Jun Park, Jong Min Kim, Meilin Liu, and Zhong Lin Wang	Angew. Chem. Int. Ed.	Vol 50, p1683 (2011)
Single-fibre-based hybridization of energy converters and storage units using graphene as electrodes	Joonho Bae, Young Jun Park, Minbaek Lee, Seung Nam Cha, Young Jin Choi, Churl Seung Lee, Jong Min Kim, Zhong Lin Wang	Advanced Materials	*Accepted*

(b) Patent

Title	Author	Status	Nation
Control of wave guiding micro/nanowire using Converted Piezoelectric Effect	, Zhong Lin Wang, Minbaek Lee	*Ongoing*	Korea